Article

Synthesis and Structure Determination of the Quaternary Zinc Nitride Halides $Zn_2NX_{1-y}X'_y$ (X, X′ = Cl, Br, I; 0 < y < 1)

Yanqing Li, Xiaohui Liu and Richard Dronskowski *

Chair of Solid-State and Quantum Chemistry, Institute of Inorganic Chemistry and JARA-FIT,
RWTH Aachen University, Aachen D-52056, Germany; yanqing.li@ac.rwth-aachen.de (Y.L.);
xiaohui.liu@ac.rwth-aachen.de (X.L.)
* Correspondence: drons@HAL9000.ac.rwth-aachen.de; Tel.: +49-241-80-93642; Fax: +49-241-80-92642

Abstract: The quaternary series $Zn_2NCl_{1-y}Br_y$ and $Zn_2NBr_{1-y}I_y$ were synthesized from solid-liquid reactions between zinc nitride and the respective zinc halides in closed ampoules, and the evolution of their crystal structures was investigated by single-crystal and powder X-ray diffraction. $Zn_2NX_{1-y}X'_y$ (X, X′ = Cl, Br, I) adopts the *anti-β*-NaFeO$_2$ motif in which each nitride ion is tetrahedrally coordinated by four zinc cations, and the halide anions are located in the voids of the skeleton formed by corner-sharing [NZn$_4$] tetrahedra. While $Zn_2NCl_{1-y}Br_y$ crystallizes in the acentric orthorhombic space group *Pna*2$_1$ (No. 33), isotypic to Zn_2NX (X = Cl, Br), the structure of $Zn_2NBr_{1-y}I_y$ is a function of the iodide concentration, namely, Zn_2NBr (*Pna*2$_1$) for low iodine content and Zn_2NI (*Pnma*) for higher ($y \geq 0.38$).

1. Introduction

In recent years, there is a growing interest in mixed-anions solids such as metal nitride halides. For these, the literature covers alkali and alkaline-earth metal nitride halides [1–16], rare-earth metal nitride halides [17–20], transition-metal nitride halides [21–24] and Millon's base [25–29]. The zinc nitride halides Zn_2NX (X = Cl, Br and I) [30,31] were synthesized from solid-liquid reactions of zinc nitride with the zinc halides, and their structures belong to the *anti-β*-NaFeO$_2$ type [32]. In addition, it has been suggested that not only the ternary alkaline-earth metal nitride halides M$_2$NX (X = F, Cl, Br and I), but also the quaternary variants M$_2$NX$_{1-y}$X′$_y$ (X, X′ = Cl, Br and I) are more complicated in terms of crystal structure. In particular, the variation of the mixed halides may change both structure and other properties [7]. After the successful synthesis of Zn_2NX (X = Cl, Br and I) [30], we became interested in such quaternary nitride halides simply because of a potential change in crystallographic symmetry. While Zn_2NX (X = Cl, Br) crystallizes in the acentric orthorhombic space group *Pna*2$_1$ (No. 33), Zn_2NI adopts the centrosymmetric space group *Pnma* (No. 62). This paper presents the synthesis and structure determination of the mixed zinc nitride halides $Zn_2NX_{1-y}X'_y$ (X, X′ = Cl, Br, I) for which a change in symmetry is to be expected at some specific stoichiometry.

2. Result and Discussion

2.1. Crystal Structure

2.1.1. Crystal Structure of $Zn_2NCl_{0.47}Br_{0.53}$

The crystal structure of $Zn_2NCl_{0.47}Br_{0.53}$ as depicted in Figure 1a corresponds to the one of Zn_2NX (X = Cl, Br) in *Pna*2_1, the *anti-β*-NaFeO$_2$ type. While there are two crystallographically independent zinc atoms, the halide anions (Cl$^-$ and Br$^-$) share the same site, and there is no indication for an ordered arrangement. Zn1 is at the center of a distorted tetrahedron with its N and Cl/Br neighbors and bond lengths of Zn1–N = 1.921(5) and 1.928(5) Å while Zn1–Cl/Br amounts to 2.606(2) and 2.823(2) Å. Zn2 also constitutes a distorted tetrahedron, the bond lengths being Zn2–N = 1.870(6) and 1.888(6) Å as well as Zn2–Cl/Br = 2.829 (2) and 2.926(2) Å.
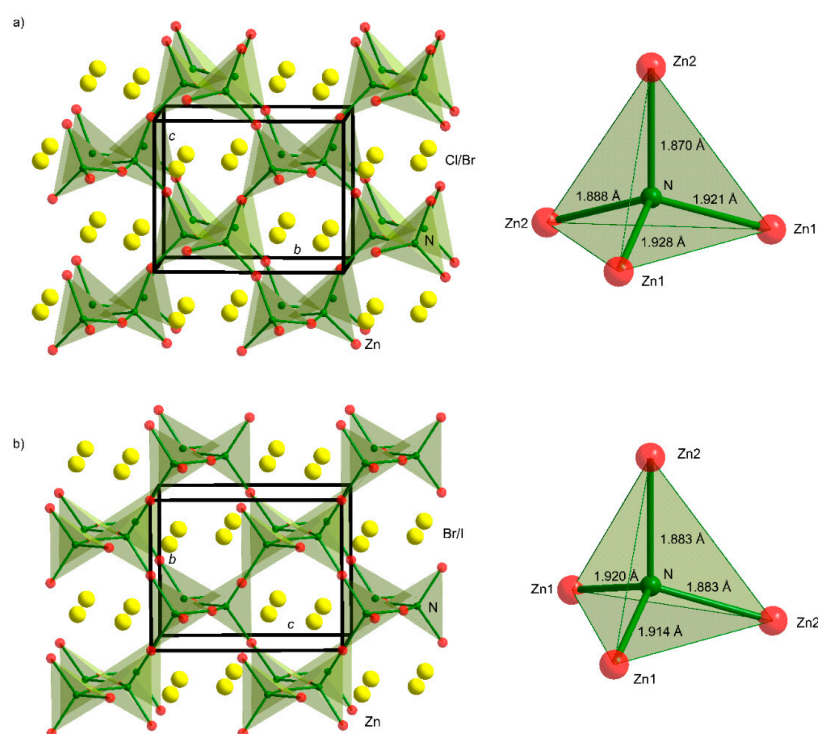

Figure 1. Polyhedral representation of [NZn$_4$] tetrahedra and the local nitrogen coordination in $Zn_2NCl_{0.47}Br_{0.53}$ (**a**) and $Zn_2NBr_{0.62}I_{0.38}$ (**b**). The Cl/Br and the Br/I anions statistically occupy the tetrahedral voids in the framework.

Likewise, the N^{3-} ion is coordinated by four zinc atoms (2 × Zn1 and 2 × Zn2), with an average Zn–N distance of 1.902 Å and Zn–N–Zn angles between 103° and 116°, in good accordance with what is known from Zn_2NX (X = Cl, Br) [30]. For further comparison, the Zn–N distance varies between 2.13 and 2.16 Å in Zn_3N_2 [33], so it is significantly larger in the binary phase than in the ternary which most probably goes back to the more ionic bonding character in the latter. This, however, is an admittedly crude guess. Also, the Zn–Cl distance is between 2.28 and 2.33 Å in ZnCl$_2$ while the mean Zn–Br distance is 2.42 Å in ZnBr$_2$ [34,35].

2.1.2. Crystal Structure of $Zn_2NBr_{0.62}I_{0.38}$

The compounds $Zn_2NBr_{0.62}I_{0.38}$, see Figure 1b, and Zn_2NI [30] are isostructural. $Zn_2NBr_{0.62}I_{0.38}$ adopts the orthorhombic space group *Pnma* in which the N^{3-} ion is coordinated by four zinc atoms, whereas the halide anions occupy the tetrahedral voids in the framework.

There are two crystallographically independent zinc atoms. Zn1 forms a distorted tetrahedron with its nitrogen, bromide, and iodide neighbors, with bond lengths of Zn1–N = 1.914(5) Å and 1.920(5) Å while Zn1–Br/I = 2.758(2) Å and Zn1–Br/I = 3.149(2) Å. Zn2 is at the center of a distorted tetrahedron with Zn2–N = 1.883(3) Å (twice) and Zn2–Br/I = 3.188 (2) Å (also twice). The N^{3-} ions are tetrahedrally coordinated by four zinc atoms with an average Zn–N = 1.90 Å; the Zn−N−Zn angles vary between 105° and 117°. For comparison, the average Zn–N distance is 1.90 Å for Zn_2NBr and 1.92 Å for Zn_2NI. Also, the Zn–N–Zn angles are 104°–116° in Zn_2NBr and 105°–117° in Zn_2NI. We also note that the Zn–I distance is 2.58–2.68 Å in ZnI_2 [36].

Owing to the increasing halide radius, the Zn–X distances enlarge in going from Cl to I. The halide anions are located in the voids resulting from the corner-sharing $[NZn_4]$ tetrahedral framework. The voids occupied by Cl/Br (N–Zn2–N is not linear) are smaller than those occupied by Br/I (N–Zn2–N strictly linear). Hence, the crystal packing of $Zn_2NBr_{1-y}I_y$ exhibits a higher symmetry than the one of $Zn_2NCl_{1-y}Br_y$ for $y \geq 0.38$ or even slightly lower.

2.2. Structure Discussion of $Zn_2NX_{1-y}X'_y$ (X, X' = Cl, Br, I; 0 < y < 1)

PXRD patterns of the quaternary zinc nitride halides are presented in Figure 2. There is an obvious shift of peaks to lower 2θ with increasing halide radii, as expected. One also witnesses tiny amounts of ZnO either resulting from the starting material Zn_3N_2 or from the quartz tube. Within the $Zn_2NBr_{1-y}I_y$ system, see Figure 2b, space group $Pna2_1$ (the one of Zn_2NBr) and $Pnma$ (the one of Zn_2NI) cannot be distinguished for trivial crystallographic reasons.
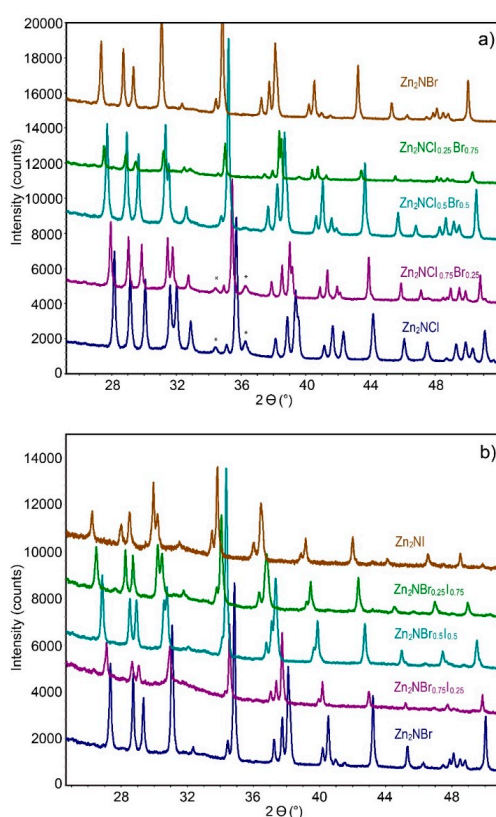

Figure 2. PXRD patterns of zinc nitride halides $Zn_2NCl_{1-y}Br_y$ (**a**) and $Zn_2NBr_{1-y}I_y$ (**b**) with $0 \leq y \leq 1$. Two samples $Zn_2NCl_{0.75}Br_{0.25}$ and Zn_2NCl within (**a**) contain small amount ZnO (asterisks).

Figure 3 displays the course of the lattice parameters and the unit cell volume (all taken from the powder, not the single-crystal data) against the bromide and iodide content in the $Zn_2NX_{1-y}X'_y$ system. For $Zn_2NCl_{1-y}Br_y$, *a*, *b*, *c*, and *V* increase linearly with the bromide content, see Figure 3a.

For $Zn_2NBr_{1-y}I_y$, the behavior is different, as shown in Figure 3b: *b* and *c* increase linearly with the iodide content but *a* first increases slightly for small iodide contents, followed by a sharper increase for larger iodine contents. This effect mirrors the structural change of the $Zn_2NBr_{1-y}I_y$ system in going from the acentric $Pna2_1$ to the centric $Pnma$ space group which, according to the single-crystal data, sets in at about $y = 0.38$, possibly even slightly earlier than that.
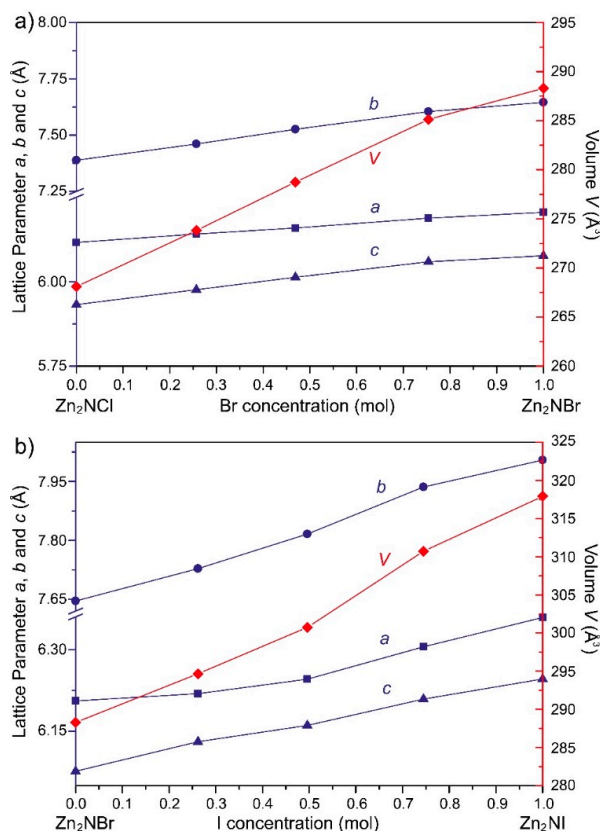

Figure 3. Course of the lattice parameters *a*, *b*, and *c* (left and blue) and volume *V* (right and red) based on XRPD data as a function of the bromide content for $Zn_2NCl_{1-y}Br_y$ (**a**) and the iodide content for $Zn_2NBr_{1-y}I_y$ (**b**).

3. Experimental

3.1. Synthesis of $Zn_2NX_{1-y}X'_y$ (X, X' = Cl, Br, I; 0 < y < 1)

Because the starting materials are air and moisture sensitive, all manipulations were carried out under a continuously purified and monitored argon atmosphere in a glove-box (H_2O and O_2 below 1 ppm) or under vacuum. The quaternary zinc nitride halides were prepared from solid–liquid reactions. The starting materials, dark gray Zn_3N_2 (Alfa, Karlsruhe, Germany, 99%) and white $ZnCl_2$ (Alfa, 99.99%; m.p.: 283 °C), $ZnBr_2$ (Alfa, 99.999%; m.p.: 394 °C), or ZnI_2 (Alfa, 99.995%; m.p.: 446 °C) were thoroughly mixed using a 1:(1 − *y*):*y* molar ratio. For X = Cl, X' = Br or X = Br, X' = I, the ratio of *y* was varied from 0 to 1 in increments of 0.25. The mixture was loaded in a quartz tube which was then sealed under vacuum. The ampoule was heated and kept at a temperature of 550 °C for 20 h. The reaction follows the simple equation:

$$Zn_3N_{2(s)} + (1 - y)\ ZnX_{2(l)} + y\ ZnX'_{2(l)} \rightarrow 2\ Zn_2NX_{1-y}X'_{y(s)} \tag{1}$$
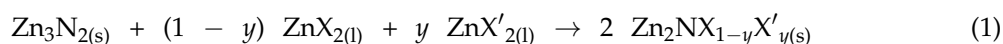
Pale white powders of $Zn_2NCl_{1-y}Br_y$ and $Zn_2NBr_{1-y}I_y$ were obtained and checked by X-ray powder diffraction (XRPD). Colorless single crystals of $Zn_2NCl_{0.47}Br_{0.53}$ and $Zn_2NBr_{0.62}I_{0.38}$ were also

obtained by the reaction of Zn_3N_2 with the respective ZnX_2 at temperatures from 550 to 600 °C for about three days. However, any attempts to synthesize $Zn_2NCl_{1-y}I_y$ were unsuccessful.

Quaternary zinc nitride halides are stable in dry air for several hours, thereby resembling the ternary zinc nitride halides.

3.2. X-ray Crystallography

Single crystals of $Zn_2NCl_{0.47}Br_{0.53}$ and $Zn_2NBr_{0.62}I_{0.38}$ were fixed on a glass fiber in air. The single-crystal data were collected at 293(2) K with a Bruker SMART APEX CCD diffractometer (Bruker AXS Inc., Madison, WI, USA) using monochromatic Mo-Kα radiation. The collection and reduction of the data were implemented with the Bruker Suite software package [37,38]. An empirical absorption correction was carried out with SADABS.

The structures of $Zn_2NCl_{0.47}Br_{0.53}$ and $Zn_2NBr_{0.62}I_{0.38}$ were solved by analogy with the ternary phases and refined by full-matrix least-squares techniques on the basis of intensities with SHELXL [37,38]. Undoubtedly, $Zn_2NCl_{0.47}Br_{0.53}$ crystallizes in the acentric space group *Pna*2_1 (No. 33) and is isotypic with Zn_2NX (X = Cl, Br). $Zn_2NBr_{0.62}I_{0.38}$, however, crystallizes in the centrosymmetric space group *Pnma* (No. 62) and is isotypic with Zn_2NI. The halide contents result from the single-crystal refinements which are more reliable in terms of stoichiometry.

The powder X-ray diffraction data of $Zn_2NX_{1-y}X'_y$ (X, X' = Cl, Br, I) were recorded at room temperature by means of a calibrated Huber Image Plate (G 670) powder diffractometer (Rimsting, Germany) (Cu-Kα_1 radiation, 6°–100° in 2θ) with a flat-sample holder. The background was manually subtracted by linear interpolation, and the FULLPROF program package [39] was used for Rietveld refinements using a pseudo-Voigt profile function. The final structural models of $Zn_2NCl_{0.47}Br_{0.53}$ and $Zn_2NBr_{0.62}I_{0.38}$ derived from single-crystal XRD were fully confirmed from the Rietveld data, as depicted in Figure 4.

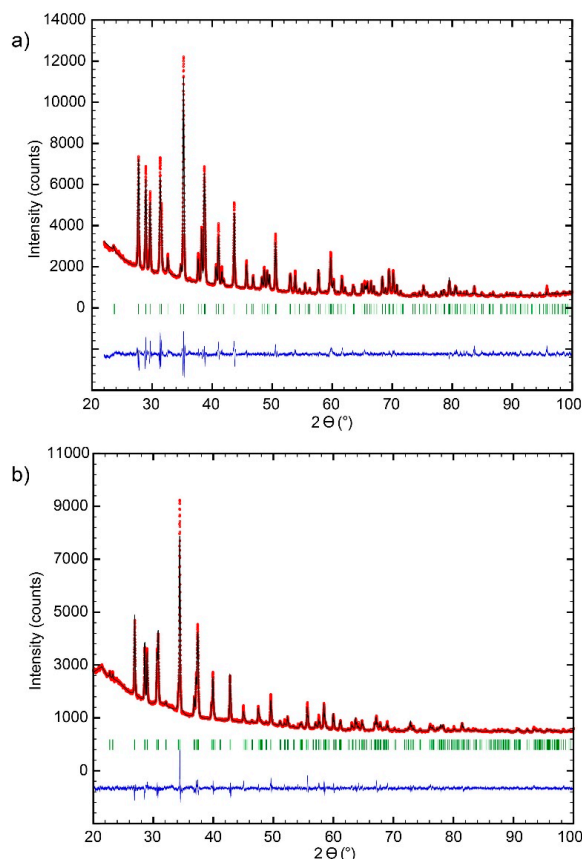**Figure 4.** Rietveld refinement of the X-ray powder pattern of $Zn_2NCl_{0.47}Br_{0.53}$ (**a**) and $Zn_2NBr_{0.62}I_{0.38}$ (**b**) showing measured and fitted intensities (**red/black**), the position of the Bragg peaks (**green**) and the difference curve (**blue**).

Details of the crystallographic data collection and structure refinement are given in Table 1. Lattice parameters, refined atomic coordinates, equivalent isotropic displacement parameters, and anisotropic displacement parameters are listed in Tables 2–4. Selected bond distances and angles are presented in Table 5. Further information in the form of CIF data has been deposited at Fachinformationszentrum Karlsruhe, 76344 Eggenstein-Leopoldshafen, Germany, and may be obtained from there using the depository CSD numbers 431875 ($Zn_2NCl_{0.47}Br_{0.53}$) and 431876 ($Zn_2NBr_{0.62}I_{0.38}$), respectively.

Table 1. Crystal data and details of the structural refinements of $Zn_2NCl_{0.47}Br_{0.53}$ and $Zn_2NBr_{0.62}I_{0.38}$.

Formula	$Zn_2NCl_{0.47}Br_{0.53}$	$Zn_2NBr_{0.62}I_{0.38}$
Formula weight (g/mol)	203.87	242.55
Color and form	colorless block	colorless block
Temperature (K)	293(2)	293(2)
Crystal system	orthorhombic	orthorhombic
Space group; Z	$Pna2_1$ (No. 33); 4	$Pnma$ (No. 62); 4
a (Å)	6.168(2)	6.249(4)
b (Å)	7.538(3)	6.164(4)
c (Å)	6.026(2)	7.824(5)
Cell volume ($Å^3$)	280.17(18)	301.4(3)
Calculated density (g/cm^3)	4.833	5.345
Crystal size (mm^3)	$0.03 \times 0.03 \times 0.01$	$0.05 \times 0.04 \times 0.01$
θ range (deg)	5.45–32.83	5.21–33.36
Index ranges	$-8 \leq h \leq 9$	$-7 \leq h \leq 9$
	$-8 \leq k \leq 11$	$-9 \leq k \leq 9$
	$-8 \leq l \leq 9$	$-12 \leq l \leq 6$
Reflections collected	2455	2215
Indep. reflections, R_{int}	824, 0.0366	585, 0.0326
Restraints; parameters	1; 38	0; 27
Goodness-of-fit	1.097	1.177
$R_1[I > 2\sigma(I)]$, w$R(I)$	0.0371, 0.0867	0.0428, 0.1147
largest diff. peak; hole ($e/Å^3$)	1.136; -1.147	2.896; -2.869

Table 2. Lattice parameter for $Zn_2NX_{1-y}X'_y$ (X, X' = Cl, Br, I; 0 < y < 1).

Lattice Parameter	Zn_2NCl [30]	$Zn_2NCl_{0.47}Br_{0.53}$	Zn_2NBr [30]	$Zn_2NBr_{0.62}I_{0.38}$	Zn_2NI [30]
a	6.1241(9)	6.168(2)	6.2149(9)	6.249(4)	6.3590(13)
b	7.3885(11)	7.538(3)	7.6529(11)	6.164(4)	6.2592(12)
c	5.9362(9)	6.026(2)	6.0859(8)	7.824(5)	7.9549(16)
V	268.60(7)	280.17(18)	289.46(7)	301.4(3)	316.30(11)

Table 3. Refined atomic coordinates and equivalent isotropic displacement parameters for $Zn_2NCl_{0.47}Br_{0.53}$ and $Zn_2NBr_{0.62}I_{0.38}$.

Atom	Wyckoff Site	x	y	z	U_{eq} ($Å^2$)	Occ (X, X')
$Zn_2NCl_{0.47}Br_{0.53}$						
Zn1	4a	0.87415(12)	0.82228(12)	0.64994(16)	0.0204(2)	
Zn2	4a	0.97750(14)	0.46071(15)	0.47667(16)	0.0244(2)	
N	4a	0.9284(7)	0.3733(7)	0.1907(10)	0.0112(8)	
Cl	4a	0.8107(13)	0.12201(12)	0.68891(14)	0.0157(3)	0.467(8)
Br	4a	-	-	-	-	0.533(8)
$Zn_2NBr_{0.62}I_{0.38}$						
Zn1	4c	0.13822(12)	3/4	0.31289(12)	0.0222(3)	
Zn2	4a	0	0	0	0.0318(4)	
N	4c	0.0644(8)	1/4	0.8716(7)	0.0108(9)	
I	4c	0.92075(8)	3/4	0.61964(7)	0.0173(3)	0.380(12)
Br	4c	-	-	-	-	0.620(12)

Table 4. Anisotropic displacement parameters (Å^2) for $Zn_2NCl_{0.47}Br_{0.53}$ and $Zn_2NBr_{0.62}I_{0.38}$.

Atom	U_{11}	U_{22}	U_{33}	U_{12}	U_{13}	U_{23}
$Zn_2NCl_{0.47}Br_{0.53}$						
Zn1	0.0123(3)	0.0198(4)	0.0291(4)	0.0049(3)	0.0010(3)	0.0006(3)
Zn2	0.0234(4)	0.0287(5)	0.0211(4)	0.0012(4)	−0.0058(3)	−0.0120(4)
N	0.0077(16)	0.015(2)	0.0108(19)	−0.0010(16)	0.0012(16)	0.0016(19)
Cl	0.0152(4)	0.0158(4)	0.0162(4)	−0.0004(3)	0.0004(3)	−0.0002(3)
Br	0.0152(4)	0.0158(4)	0.0162(4)	−0.0004(3)	0.0004(3)	−0.0002(3)
$Zn_2NBr_{0.62}I_{0.38}$						
Zn1	0.0113(5)	0.0327(5)	0.0226(5)	0	−0.0053(3)	0
Zn2	0.0284(5)	0.0290(5)	0.0380(6)	−0.0137(4)	−0.0087(4)	0.0218(4)
N	0.0078(17)	0.012(2)	0.013(2)	0	0.0002(15)	0
I	0.0148(4)	0.0170(4)	0.0200(4)	0	0.00094(17)	0
Br	0.0148(4)	0.0170(4)	0.0200(4)	0	0.00094(17)	0

Table 5. Selected bond distances (Å) and angles (°) in $Zn_2NCl_{0.47}Br_{0.53}$ and $Zn_2NBr_{0.62}I_{0.38}$.

$Zn_2NCl_{0.47}Br_{0.53}$	Distance/Angle	$Zn_2NBr_{0.62}I_{0.38}$	Distance/Angle
Zn1–N	1.921(5)	Zn1–N	1.914(5)
Zn1–N	1.928(5)	Zn1–N	1.920(5)
Zn1–Cl/Br	2.6055(15)	Zn1–Br/I	2.7579(17)
Zn1–Cl/Br	2.8230(17)	Zn1–Br/I	3.1487(19)
Zn2–N	1.870(6)	Zn2–N	1.883(3)
Zn2–N	1.888(6)	Zn2–N	1.883(3)
Zn2–Cl/Br	2.8292(15)	Zn2–Br/I	3.1881(15)
Zn2–Cl/Br	2.9261(17)	Zn2–Br/I	3.1881(15)
N–Zn1–N	138.6(2)	N–Zn1–N	145.14(16)
N–Zn2–N	155.9(2)	N–Zn2–N	180
Zn2–N–Zn2	110.2(3)	Zn2–N–Zn2	109.8(3)
Zn2–N–Zn1	110.2(3)	Zn2–N–Zn1	109.60(17)
Zn2–N–Zn1	110.1(3)	Zn2–N–Zn1	109.60(17)
Zn2–N–Zn1	106.5(3)	Zn2–N–Zn1	105.08(17)
Zn2–N–Zn1	103.0(3)	Zn2–N–Zn1	105.08(17)
Zn1–N–Zn1	116.4(3)	Zn1–N–Zn1	117.4(3)

4. Conclusions

The quaternary series $Zn_2NCl_{1-y}Br_y$ and $Zn_2NBr_{1-y}I_y$ were synthesized and their crystal structures were investigated by single-crystal and powder X-ray diffraction. $Zn_2NX_{1-y}X'_y$ (X, X′ = Cl, Br, I) follow the *anti-β*-NaFeO$_2$ motif. Each N^{3-} is tetrahedrally coordinated by four zinc atoms, and the X$^-$ anions are located in the voids of the skeleton formed by corner-sharing [NZn$_4$] tetrahedra. While $Zn_2NCl_{1-y}Br_y$ is isotypic with Zn_2NX (X = Cl, Br) and crystallizes in the acentric orthorhombic space group *Pna*2$_1$, the $Zn_2NBr_{1-y}I_y$ series changes its space groups as a function of the iodide content, that is, *Pna*2$_1$ for low I content and *Pnma* for higher, namely $y \geq 0.38$ or even slightly lower according to single-crystal data.

References

1. Marx, R.; Mayer, H.-M. Preparation and Crystal Structure of Ordered and Disordered Lithium Nitride Dichloride, Li$_5$NCl$_2$. *J. Solid State Chem.* **1997**, *130*, 90–96. [CrossRef]

2. Marx, R. Preparation and Crystal Structure of Lithium Nitride Chloride Li$_4$NCl. *J. Solid State Chem.* **1997**, *128*, 241–246. [CrossRef]

3.   Andersson, S. Magnesium nitride fluorides. *J. Solid State Chem.* **1970**, *1*, 306–309. [CrossRef]

4.   Brogan, M.A.; Hughes, R.W.; Smith, R.I.; Gregory, D.H. Structural studies of magnesium nitride fluorides by powder neutron diffraction. *J. Solid State Chem.* **2012**, *185*, 213–218. [CrossRef]

5.   Li, Y.; George, J.; Liu, X.; Dronskowski, R. Synthesis, Structure Determination and Electronic Structure of Magnesium Nitride Chloride, Mg_2NCl. *Z. Anorg. Allg. Chem.* **2015**, *641*, 266–269. [CrossRef]

6.   Reckeweg, O.; DiSalvo, F.J. Alkaline earth metal nitride compounds with the composition M_2NX (M = Ca, Sr, Ba; X = □, H, Cl or Br). *Solid State Sci.* **2002**, *4*, 575–584. [CrossRef]

7.   Bowman, A.; Smith, R.I.; Gregory, D.H. Ternary and quaternary layered nitride halides, $Ca_2N(X, X')$ (*X, X'* = Cl, Br, I): Evolution of structure with composition. *J. Solid State Chem.* **2005**, *178*, 1807–1817. [CrossRef]

8.   Bailey, A.S.; Hughes, R.W.; Hubberstey, P.; Ritter, C.; Smith, R.I.; Gregory, D.H. New Ternary and Quaternary Barium Nitride Halides; Synthesis and Crystal Chemistry. *Inorg. Chem.* **2011**, *50*, 9545–9553. [CrossRef] [PubMed]

9.   Ehrlich, P.; Linz, W.; Seifert, H.J. Nitridfluoride der schweren Erdalkalimetalle. *Naturwissenschaften* **1971**, *58*, 219–220. [CrossRef]

10. Nicklow, R.A.; Wagner, T.R.; Raymond, C.C. Preparation and Single-Crystal Structure Analysis of Ca_2NF. *J. Solid State Chem.* **2001**, *160*, 134–138. [CrossRef]

11. Jack, D.R.; Zeller, M.; Wagner, T.R. Doubled-cubic Ca_2NF. *Acta Crystallogr.* **2005**, *C61*, i6–i8.

12. Wagner, T.R. Preparation and single-crystal structure analysis of Sr_2NF. *J. Solid State Chem.* **2002**, *169*, 13–18. [CrossRef]

13. Seibel, H.; Wagner, T.R. Preparation and crystal structure of Ba_2NF. *J. Solid State Chem.* **2004**, *177*, 2772–2776. [CrossRef]

14. Hadenfeldt, C.; Herdejürgen, H. Darstellung und Kristallstruktur der Calciumnitridhalogenide Ca_2NCl und Ca_2NBr. *Z. Anorg. Allg. Chem.* **1987**, *545*, 177–183. [CrossRef]

15. Hadenfeldt, C.; Herdejürgen, H. Darstellung und Kristallstruktur der Calciumpnictidiodide Ca_2NI, Ca_2PI und Ca_2AsI. *Z. Anorg. Allg. Chem.* **1988**, *558*, 35–40. [CrossRef]

16. Bowman, A.; Smith, R.I.; Gregory, D.H. Synthesis and structure of the ternary and quaternary strontium nitride halides, $Sr_2N(X, X')$ (*X, X'* = Cl, Br, I). *J. Solid State Chem.* **2006**, *179*, 130–139. [CrossRef]

17. Ehrlich, G.M.; Badding, M.E.; Brese, N.E.; Trail, S.S.; DiSalvo, F.J. New cerium nitride chlorides: $Ce_6Cl_{12}N_2$ and CeNCl. *J. Alloys Compds.* **1996**, *235*, 133–134. [CrossRef]

18. Meyer, H.J.; Jones, N.L.; Corbett, J.D. A new yttrium sesquichloride nitride, β-Y_2Cl_3N, that is isostructural with the binary yttrium sesquichloride. *Inorg. Chem.* **1989**, *28*, 2635–2637. [CrossRef]

19. Schwanitz-Schüller, U.; Simon, A. Synthese und Kristallstruktur von Gd_2NCl_3. *Z. Naturforsch.* **1985**, *40b*, 705–709.

20. Schurz, C.M.; Schleid, T. Chains of *trans*-edge connected [ZM_4] tetrahedra (Z = N and O) in the lanthanide nitride chlorides M_2NCl_3 and $Na_2M_4ONCl_9$ (M = La–Nd). *J. Alloys Compds.* **2009**, *485*, 110–118. [CrossRef]

21. Yamanaka, S.; Yasunaga, T.; Yamaguchi, K.; Tagawa, M. Structure and superconductivity of the intercalation compounds of TiNCl with pyridine and alkali metals as intercalants. *J. Mater. Chem.* **2009**, *19*, 2573–2582. [CrossRef]

22. Istomin, S.Y.; Köhler, J.; Simon, A. Crystal structure of β-ZrNCl refined from X-ray powder diffraction data, electronic band structures of β-ZrNCl and superconducting LixZrNCl. *Physica C* **1999**, *319*, 219–228. [CrossRef]

23. Chen, X.; Koiwasaki, T.; Yamanaka, S. High-Pressure Synthesis and Crystal Structures of *β-M*NCl (*M* = Zr and Hf). *J. Solid State Chem.* **2001**, *159*, 80–86. [CrossRef]

24. Yamanaka, S.; Hotehama, K.-I.; Kawaji, H. Superconductivity at 25.5 K in electron-doped layered hafnium nitride. *Nature* **1998**, *392*, 580–582. [CrossRef]

25. Weiser, H.B. The Luminescence of the Iodide of Millon's Base. *J. Phys. Chem.* **1917**, *21*, 37–47. [CrossRef]

26. Lipscomb, W.N. The structure of mercuric amidochloride, $HgNH_2Cl$. *Acta Crystallogr.* **1951**, *4*, 266–268. [CrossRef]

27. Lipscomb, W.N. The structure of Millon's base and its salts. *Acta Crystallogr.* **1951**, *4*, 156–158. [CrossRef]

28. Nijssen, L.; Lipscomb, W.N. A hexagonal modification of a salt of Millon's base. *Acta Crystallogr.* **1954**, *7*, 103–106. [CrossRef]

29. Holleman, A.F.; Wiberg, E. *Inorganic chemistry*; Academic Press: San Diego, CA, USA, 2001.

30. Liu, X.; Wessel, C.; Pan, F.; Dronskowski, R. Synthesis and single-crystal structure determination of the zinc nitride halides Zn_2NX (X = Cl, Br, I). *J. Solid State Chem.* **2013**, *203*, 31–36. [CrossRef]

31. Marchand, R.; Lang, J. Sur la préparation d'halogénonitrures de zinc. *C. R. Hebd. Seances Acad. Sci.* **1970**, *270*, 540–542.

32. Grey, I.E.; Hill, R.J.; Hewat, A.W. A neutron powder diffraction study of the β to γ phase transformation in $NaFeO_2$. *Z. Kristallogr.* **1990**, *193*, 51–69. [CrossRef]

33. Partin, D.E.; Williams, D.J.; O'Keeffe, M. The Crystal Structures of Mg_3N_2 and Zn_3N_2. *J. Solid State Chem.* **1997**, *132*, 56–59. [CrossRef]

34. Yakel, H.L.; Brynestad, J. Refinement of the crystal structure of orthorhombic zinc chloride. *Inorg. Chem.* **1978**, *17*, 3294–3296. [CrossRef]

35. Chieh, C.; White, M.A. Crystal structure of anhydrous zinc bromide. *Z. Kristallogr.* **1984**, *166*, 189–197.

36. Fourcroy, P.H.; Carre, D.; Rivet, J. Structure cristalline de l'iodure de zinc ZnI_2. *Acta Crystallogr.* **1978**, *B34*, 3160–3162. [CrossRef]

37. *Bruker APEX2*, version 1.08; Bruker AXS Inc.: Madison, WI, USA, 2005.

38. Sheldrick, G.M. A short history of SHELX. *Acta Crystallogr.* **2008**, *A64*, 112–122. [CrossRef] [PubMed]

39. Rodríguez-Carvajal, J. Recent advances in magnetic structure determination by neutron powder diffraction. *Physica B* **1993**, *192*, 55–69. [CrossRef]